Draft version May 3, 2017
Typeset using LaTeX **preprint** style in AASTeX61

A SHORT-TERM ESPERTA-BASED FORECAST TOOL FOR MODERATE-TO-EXTREME SOLAR PROTON EVENTS

M. Laurenza,[1] T. Alberti,[2] and E. W. Cliver[3,4]

[1] *INAF-IAPS, Via del Fosso del Cavaliere, 100, I-00133, Roma, Italy*
[2] *Dipartimento di Fisica, Università della Calabria, Ponte P. Bucci, Cubo 31C, 87036, Rende (CS) Italy*
[3] *National Solar Observatory, 3665 Discovery Drive, Boulder, CO, 80303, USA*
[4] *Air Force Research Laboratory, Space Vehicles Directorate, 3550 Aberdeen Ave., Kirtland AFB, NM 87117, USA*

(Received; Revised; Accepted)

Submitted to ApJ

ABSTRACT

The ESPERTA (Empirical model for Solar Proton Event Real Time Alert) proton event forecast tool had a Probability of Detection (POD) of 62% for all the >10 MeV events with proton peak intensity ≥10 pfu (i.e., ≥S1 events, where S1 refer to minor storms on the NOAA Solar Radiation Storms scale), from 1995-2014 with a false alarm rate (FAR) of 39% and a median (minimum) warning time of ∼4.8 (0.4) h. The NOAA space weather scale includes four additional categories for proton events: moderate (S2), strong (S3), severe (S4), and extreme (S5). As S1 events have only minor impacts on HF radio propagation in the polar regions, the effective threshold for space radiation appears to be the S2 level (100 pfu), producing both biological and space operations impacts and increased effects on HF propagation in the polar regions. We modified the ESPERTA model to predict ≥S2 events and obtained a POD of 76% (41/54) and a FAR of 23% (12/53) for the 1995-2014 interval with a median (minimum) warning time of ∼1.2 (∼0.2) h based on predictions made at the time of the S1 threshold crossing. The improved performance of ESPERTA for S2 events is a reflection of the big flare syndrome where the association of the various manifestations of eruptive solar flares increases as one considers increasingly large events. For example, coronal mass ejection speed, a key indicator of event energy, has a median value of 1289 km/s for S1 events from 1995-2014 vs. 1748 km/s for S2 events.

Keywords: methods: data analysis - Sun: activity - Sun: flares - Sun: particle emission - Sun: radio radiation - Sun: X-rays, gamma rays

Corresponding author: Monica Laurenza
monica.laurenza@iaps.inaf.it

1. INTRODUCTION

Accurately predicting solar activity is notoriously diffcult, be it on solar cycle or short-term (hours) time scales (e.g. Pesnell 2012; Barnes et al. 2016). The ultimate test of our understanding of solar activity will be reliable forecasts of the timing of solar eruptions and the severity of their terrestrial impacts. Such expertise lies in the future. More promising now are techniques that exploit the disturbance propagation delay between eruptive flares and their magnetic or proton impacts at 1 au. The chief hurdle for accurate predictions of geomagnetic storms using this approach is the difficulty of determining the orientation of the magnetic eld of the responsible coronal mass ejection (CME), although progress is being made on this front (Marubashi et al. 2015). For solar proton events (SPEs), the primary obstacle for reliable warning of impending events is the rapid determination of CME speed and identication of shock formation (the principal determinants of the acceleration of energetic protons observed in space; Reames 1999, 2013, 2017; Cliver 2016), given that the lowest energy protons of interest (∼10 MeV) propagate to Earth in ∼1 hour.

During the last decade, with the increasing focus on the applied (or space weather) aspects of solar-terrestrial physics (US National Academy of Sciences [1] 2008; Lloyds[2] of London 2010; JASON[3] 2011; and the UK Royal Academy of Engineering[4] 2013, among others), a number of methods (e.g., Posner 2007; Kalher et al. 2007; Balch 2008; Laurenza et al. 2009; Núñez 2011; Papaioannou et al. 2015; Winter & Ledbetter 2015; Alberti et al. 2017; St. Cyr et al. 2017) have been investigated to provide advance warning of SPEs with intensities for a threshold of 10 proton flux units (pfu; 1 pfu = 1 pr cm^{-2} s^{-1} sr^{-1}). Such SPEs are designated "minor" (or S1) events on the NOAA Space Weather Prediction Center (SWPC) scale of Solar Radiation Storms (Table 1 http://www.swpc.noaa.gov/noaa-scales-explanation). The utility of such forecasts is measured by the percentage of such events that are predicted, the false alarm rate, and the lead warning time. Alberti et al. (2017) recently validated the ESPERTA (Empirical model for Solar Proton Event Real Time Alert, Laurenza et al. (2009); see also Laurenza et al. (2007); Storini et al. (2008); Signoretti et al. (2011)) proton prediction tool for the interval from 2006-2014, outside of the 1995-2005 period for which it was developed. The ESPERTA prediction parameters they obtained for this interval are fairly typical for such SPE forecast methods: Probability of Detection (POD) = 59% (19/32); False Alarm Rate (FAR) = 30% (8/27); median (minimum) warning time = ∼2 (0.4) h (range from 0.4 to 35.9 h) and are similar to those determined by Laurenza et al. (2009) for the 1995-2005 development period. A prime focus of the ESPERTA model was to provide timely warnings, within 10 minutes of the flare soft X-ray maximum. Within this time constraint it is difficult to condently determine CME speeds and identify the radio type II bursts that signal the existence of coronal shocks. Thus ESPERTA is based on input flare data (flare location, flare 1-8 $\AA$ soft X-ray (SXR) fluence, and flare 1 MHz radio fluence) that is, or could be made, available in real time. These three parameters provide information on proton propagation, solar event energy, and particle escape, respectively. ESPERTA forecasts are only made for SXR flares of ≥ M2 class (peak intensity ≥ 2 x 10^{-5} W m^{-2}). Table 1 shows that SWPC has four additional warning levels for proton storms beyond the S1 (minor) proton event classication. These are: S2 (moderate; 10^2 pfu); S3 (strong; 10^3 pfu), S4 (severe; 10^4 pfu), and

[1] National Academy of Sciences: https://www.nap.edu/catalog/12507/severe-space-weather-events-understanding-societal-and-economic-impacts-a

[2] Lloyds: http://www.lloyds.com/~/media/lloyds/reports/360/360%20space%20weather/7311_lloyds_360_space%20weather_03.pdf;

[3] JASON: https://fas.org/irp/agency/dod/jason/spaceweather.pdf

[4] Royal Academy: http://www.raeng.org.uk/publications/reports/space-weather-full-report

Table 1. NOAA Space Weather Scales.

Solar Radiation Storms			Flux level of ≥ 10 Mev particles (ions)	Number of events when flux level was met
S5	Extreme	Biological: unavoidable high radiation hazard to astronauts on EVA (extra-vehicular activity); passengers and crew in high-flying aircraft at high latitudes may be exposed to radiation risk. Satellite operations: satellites may be rendered useless, memory impacts can cause loss of control, may cause serious noise in image data, star-trackers may be unable to locate sources; permanent damage to solar panels possible. Other systems: complete blackout of HF (high frequency) communications possible through the polar regions, and position errors make navigation operations extremely difficult.	10^5	Fewer than 1 per cycle
S4	Severe	Biological: unavoidable radiation hazard to astronauts on EVA; passengers and crew in high-flying aircraft at high latitudes may be exposed to radiation risk. Satellite operations: may experience memory device problems and noise on imaging systems; star-trackers problems may cause orientation problems, and solar panel efficiency can be degraded. Other systems: blackout of HF radio communications through the polar regions, and increased navigation errors over several days are likely.	10^4	3 per cycle
S3	Strong	Biological: radiation hazard avoidance recommended for astronauts on EVA; passengers and crew in high-flying aircraft at high latitudes may be exposed to radiation risk. Satellite operations: single-event upsets, noise in imaging systems, and slight reduction of efficiency in solar panel are likely. Other systems: degraded HF radio propagation through the polar regions and navigation position errors likely.	10^3	10 per cycle
S2	Moderate	Biological: passengers and crew in high-flying aircraft at high latitudes may be exposed to elevated radiation risk. Satellite operations: infrequent single-event upsets possible. Other systems: effects on HF propagation through the polar regions, and navigation at polar cap locations possibly affected.	10^2	25 per cycle
S1	Minor	Biological: none Satellite operations: none. Other systems: minor impacts on HF radio in the polar regions.	10	50 per cycle

S5 (extreme; 10^5 pfu). The listed effects for S1 events are relatively benign. Only at the S2 level are biological and satellite operations effects sensible, in addition to increased (over S1) HF propagation effects in the polar regions. Thus, in this study we will evaluate the ESPERTA model for ≥S2 SPEs which are an order of magnitude, or more, larger than the S1 events. Our list of ≥S2 events with flare, CME, and coronal shock associations for the 1995-2015 interval analysis is presented in Section 2 and the results are summarized and discussed in Section 3.

2. DATABASE

We compiled a list of ≥S2 SPEs from 1995-2014 by beginning with the published lists of ≥S1 events from Laurenza et al. (2009) and Alberti et al. (2017) for 1995-2005 and 2006-2014, respectively. We surveyed 5-min proton data obtained from the Geostationary Operational Environmental Satellite (GOES) spacecraft series during their operational time, using the satellite with the highest peak flux for each SPE (http://cdaweb.nasa.gov). As is the case for the identification of ≥S1 events, we required that ≥S2 events meet or exceed the S2 threshold for three consecutive 5-min intervals. Of the 129 ≥S1 events identified by Laurenza et al. (2009) and Alberti et al. (2017), about half (59) were ≥S2 events. In Table 2, we list flare, CME, and forecast data for each of these 59 events in the following columns: (1) event number, (2) flare date, (3) peak time of the SXR burst, (4) SXR burst class (in terms of the GOES peak 1-8 $\AA$ intensity, defined as follows: classes C1-9, M1-9,

Table 2. $\geq$ 100 pfu SEP Flare List (1995-2014).

Event Number	SXR Date	SXR Peak Time (hh:mm)	SXR Class	Hα Location	SXR Fluence (J/m^2)	SXR Flag	Radio Fluence (sfu x min)	Radio Frequency (kHz)	CME Linear Speed (km/s)	SWPC Radiation Class	S1 Crossing Time (min)	S2 Crossing Time (min)	SEP Forecast Result
1	1997 Nov 6	11:55	X9	S18W63	3.61e-1	7	1.87e+7	940	1556	S2	60	195	Hit
2	1998 Apr 20	10:21	M1	W115					1863	S3			
3	1998 May 2	13:42	X1	S15W15	7.37e-2	5	2.14e+7	940	938	S2	23	103	Hit
4	1998 May 6	08:09	X2	S11W65	2.35e-1	5	8.85e+6	940	1099	S2	21	66	Hit
5	1998 Aug 24	22:12	X1	N35E09	1.88e-1	5	1.79e+7	940		S2	83	213	Hit
6	1998 Sep 30	13:48	M3	N23W81	9.61e-2	2	7.09e+5	940		S3			Miss
7	1998 Nov 14	05:18	C2	W130						S2			
8	2000 Jul 14	10:23	X6	N22W07	1.35e+0	5	1.20e+7	940	1674	S4	12	37	Hit
9	2000 Sep 12	12:12	M1	S19W08	2.94e-2	1	5.43e+6	940	1550	S2			MISS
10	2000 Nov 8	23:37	M8	N10W77	3.36e-1	3	4.51e+6	940	1738	S4	3	28	Hit
11	2000 Nov 25	01:31	M8	N07E50	2.66e-1	5	1.69e+6	940	1289	S2			Miss
12	2001 Apr 2	21:50	X18	N18W82	1.62e+0	5	2.75e+6	940	2505	S3	100	190	Hit
13	2001 Apr 10	05:26	X2	S23W09	3.66e-1	5	9.50e+6	940	2411	S2	194	484	Hit
14	2001 Apr 15	13:50	X16	S20W85	6.20e-1	7	8.77e+6	940	1199	S2	10	25	Hit
15	2001 Apr 18	02:14	C2	W120					2465	S2			
16	2001 Aug 15	23:55	<C1	W180						S2			
17	2001 Sep 24	10:35	X3	S12E29	1.09e+0	3	1.48e+6	940	2402	S4	90	150	Hit
18	2001 Oct 1	05:15	M9	S22W85	7.56e-2	5	1.12e+5	940	1405	S3			Miss
19	2001 Nov 4	16:19	X1	N07W19	2.76e-1	2	1.36e+7	940	1810	S4	36	56	Hit
20	2001 Nov 22	23:27	X1	S15W34	4.68e-1	3	1.38e+5	940	1437	S4	8	148	Hit
21	2001 Dec 26	05:36	M7	N08W54	6.30e-1	4	1.14e+6	940	1446	S2	19	49	Hit
22	2001 Dec 28	20:42	X3	S26E95	2.92e+0	4	4.43e+6	940	2216	S2	243	783	Hit
23	2002 Apr 21	01:47	X1	S14W84	7.82e-1	3	4.51e+6	940	2393	S3	28	38	Hit
24	2002 May 22	03:48	C5	S22W53	1.82e-2	1	2.02e+6	940	1557	S2			MISS
25	2002 Jul 15	20:08	X3	N19W01	1.49e-1	7	9.81e+6	940	1151	S2	892	2402	Hit
26	2002 Aug 24	01:11	X3	S02W81	5.75e-1	5	Cal	940	1913	S2			
27	2002 Sep 5	17:04	C5	N09E28	2.49e-2	3	2.34e+5	940	1748	S2			MISS
28	2002 Nov 9	13:23	M5	S12W29	5.52e-2	5	8.14e+6	940	1838	S2			Miss
29	2003 May 28	00:27	X4	S07W21	3.12e-1	5	7.20e+6	940	1366	S2	1383	2323	Hit
30	2003 Oct 26	18:11	X1	N02W38	3.83e-1	1	1.43e+6	916	1537	S2	4	34	Hit
31	2003 Oct 28	11:10	X18	S16E07	1.96e+0	5	2.16e+7	916	1057	S4	55	85	Hit
32	2003 Oct 29	20:49	X11	S15W02	9.80e-1	5	8.79e+6	916	2029	S3	0	151	Hit
33	2003 Nov 2	17:25	X9	S14W56	1.09e+0	5	2.70e+6	916	2036	S3	15	40	Hit
34	2003 Nov 4	19:44	X18	S19W83	2.65e+0	1	9.53e+5	916	2657	S2	151	581	Hit
35	2004 Jul 25	15:15	M1	N08W344	3.25e-2	1	7.51e+4	940	1233	S3			MISS
36	2004 Nov 7	16:06	X2	N09W17	2.08e-1	5	1.36e+6	940	1759	S2	174	184	Hit
37	2004 Nov 10	02:13	X3	N09W49	1.68e-1	7	1.84e+6	940	3387	S2	67	217	Hit
38	2005 Jan 15	23:00	X3	N14W08	8.63e-1	2	1.01E+6	916	2861	S2	150	850	Hit
39	2005 Jan 17	09:52	X4	N14W24	7.20e-1	5	1.63e+6	916	2094	S3	0	73	Hit
40	2005 Jan 20	07:00	X8	N12W58	1.97e+0	5	1.66e+7	916	882	S3	10	60	Hit
41	2005 May 13	16:57	M8	N12E11	2.50e-1	5	1.79e+7	916	1689	S3	628	1558	Hit
42	2005 Jul 14	10:54	X1	W95	6.63e-1	3	2.65e+4	916	1423	S2			Miss
43	2005 Aug 22	17:28	M6	S12W60	2.87e-1	3	1.54e+6	916	2378	S2	238	392	Hit
44	2005 Sep 07	17:40	X18	S06E89	6.65e+0	3	1.42e+7	916	2257	S3	690	2640	Hit
45	2005 Sep 13	20:04	X1	S09E05	4.86e-1	5	1.49e+5	916	1866	S2			Miss
46	2006 Dec 5	10:35	X9	S07E79	6.12e-1	5	1.90e+6	916		S3	1760	2910	Hit
47	2006 Dec 13	02:39	X3	S05W23	5.88e-1	5	1.82e+7	916	1774	S2	31	106	Hit
48	2012 Jan 23	03:59	M8	N28W36	3.97e-2	5	5.26e+5	916	2175	S3			Miss
49	2012 Jan 27	18:37	X1	N27W71	2.33e-1	5	4.38e+6	916	2508	S2	28	103	Hit
50	2012 Mar 7	00:24	X5	N17E15	6.89e-1	5	2.19e+7	916	2684	S3	286	626	Hit
51	2012 Mar 13	17:41	M7	N18W62	2.65e-1	3	2.92e+6	916	1884	S2	29	104	Hit
52	2012 May 17	01:47	M5	N12W89	1.21e-1	5	9.08e+6	916	1582	S2	23	98	Hit
53	2012 Jul 17	17:15	M1	S17W75	1.86e-1		3.27e+5	916	958	S2			MISS
54	2013 Apr 11	07:16	M6	N09E12	7.11e-2	5	3.38e+7	916	986	S2	64	359	Hit
55	2013 May 22	13:32	M5	N15W70	1.77e-1	3	5.74e+5	916	1537	S3	48	378	Hit
56	2013 Sep 29	23:37	C1	N15W40	3.07e-3		6.94e+4	916	1025	S2			MISS
57	2014 Jan 7	18:32	X1	S15W11	2.95e-1	5	7.85e+6	916	1830	S3	83	343	Hit
58	2014 Feb 25	00:49	X4	S12E82	4.64e-1	5	6.83e+6	916	2147	S2	786	4676	Hit
59	2014 Sep 10	17:45	X1	N16W06	3.88e-1	5	3.49e+7	916	1425	S2	415	2595	Hit

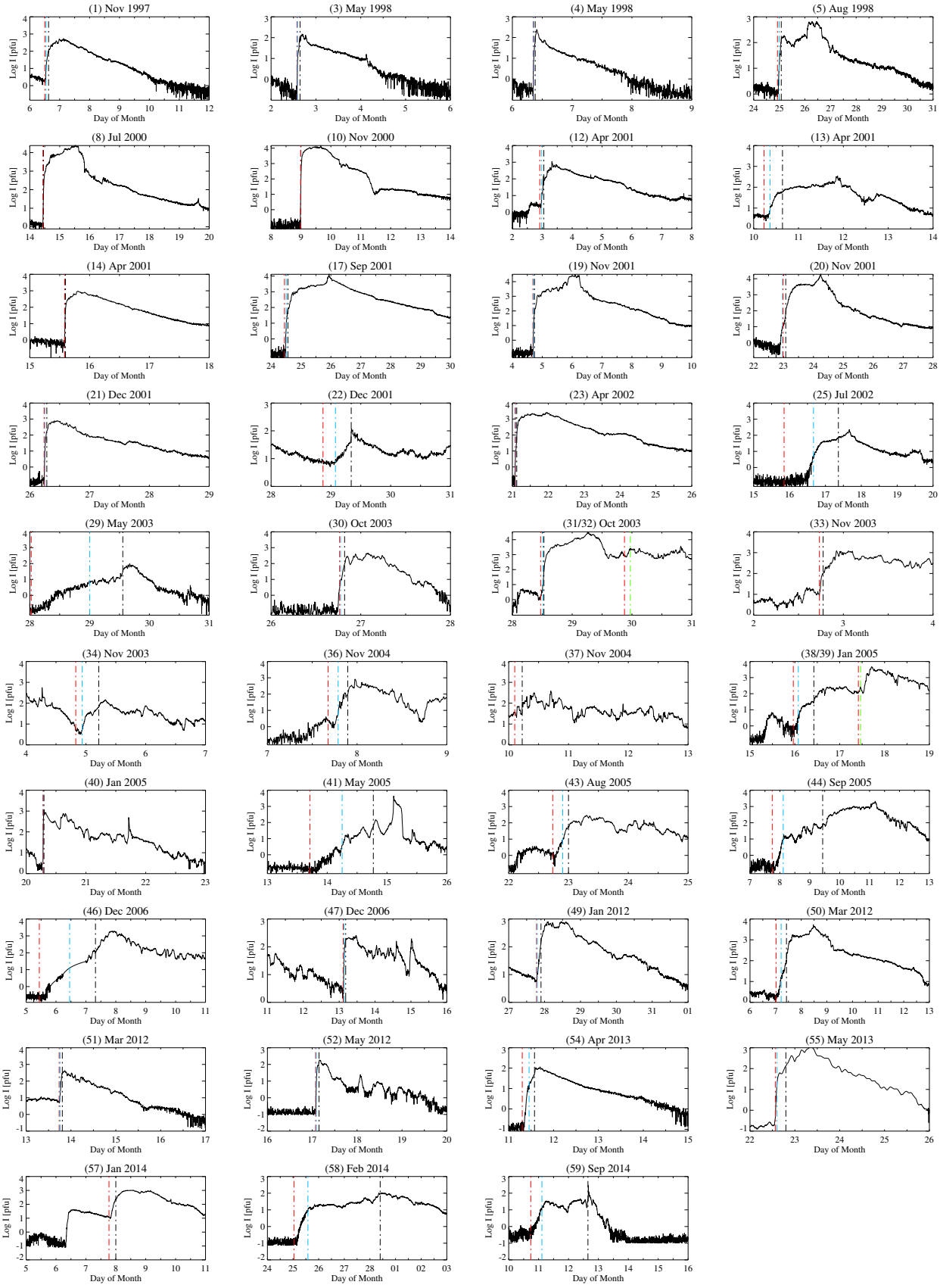

Figure 1. Intensity time profiles for the 41 "Hit" (correctly- predicted) ≥S2 >10 MeV proton events in Table 2. The vertical redline gives the time 10 minutes after the peak of the ≥M2 SXR flare, the light-blue line gives the time that the proton event intensity crossed the S1 level, and the black line gives the crossing time of the S2 event threshold.

and X1-9 correspond to flare peak intensities of 1-9$\times10^{-6}$, 1-9$\times10^{-5}$, and 1-9$\times10^{-4}$ W m^{-2}, respectively, (5) heliographic location of the associated solar eruption, (6) time-integrated SXR intensity (http://spidr.ngdc.noaa.gov/spidr/index.jsp), (7) SXR integration flag (see Laurenza et al. (2009) and Alberti et al. (2017) for the determination of both SXR and radio (Col. 8) fluences), (8) time-integrated ∼1 MHz Wind/Waves type III intensity (http://lep694.gsfc.nasa.gov/ waves/waves.html; Bougeret et al. (1995)), (9) actual (closest to 1 MHz) frequency used in Col. (8), (10) linear CME speed from SOHO/LASCO catalog (Yashiro et al. 2004; Gopalswamy et al. 2009) (11) SWPC radiation class; (12) warning time for ≥S1 events, difference between S1 threshold crossing time (end of three consecutive 5-min intervals with >10 MeV flux ≥10 pfu) and 10 min after the SXR peak time), (13) difference between the S2 threshold crossing time (end of three consecutive 5-min intervals with >10 MeV flux ≥100 pfu) and 10 min after the SXR peak time), and (14) SPE forecast result (where Hit, Miss, MISS, and blank refer to SPEs correctly predicted (41 cases), SPEs events with associated front-side or far-side ≥M2 SXR flares that were not predicted (7 cases), SPEs events with associated front-side <M2 SXR flares (6 cases; no prediction made), and SPEs associated with backside flares with SXR peaks <M2 or incomplete flare observations (5 cases; not included in the forecast statistics). Figure 1 gives plots of the >10 MeV SPE time profiles (highest GOES data) for each of the 41 S2 "hit" events in Table 2. The vertical redline gives the time 10 minutes after the peak of the ≥M2 SXR flare (when S1 alerts are issued), the light-blue line gives the time that the proton event intensity crossed the S1 level (i.e., the end of the third consecutive 5-min interval with intensity ≥10 pfu; also the time that the S2 alerts are issued), and the black line gives the crossing time of the S2 event threshold (end of the third consecutive 5-min interval with intensity ≥100 pfu).

3. FORECASTING ≥S1 AND ≥S2 EVENTS (1995-2014)

3.1. *ESPERTA applied to ≥S1 (≥10 pfu) events*

From 1995-2014, a number of 880 ≥M2 SXR flares were observed. A scatter plot of the ∼1 MHz radio fluence for theses flares vs. their SXR fluence (both as determined by ESPERTA algorithms from data streams ending within 10-min after the 1-8 $\AA$ peak (Laurenza et al. 2009; Alberti et al. 2017)) is given in Figure 2. The value of the probability assigned to the dashed-line contours for each of the three longitude ranges is based on the logistic regression analysis of McCullagh & Nelder (1983) (see also Silvermann 1998; Garcia 1994; Laurenza et al. 2009; Alberti et al. 2017). It can range from 0 to 1 and is selected to maximize the POD while minimizing the FAR for ESPERTA forecasts over the specified longitude range for this 20-yr time interval. The contours in Figure 2 separate SXR events for which a positive forecast of a ≥S1 event was made (events above the contour) from those for which a null event forecast was made (events below the contour). The three longitude bins contain a total of 82 colored symbols: 66 diamonds (Hits) and 20 stars ("Misses"; 21 MISSes associated with frontside <M2 flares not plotted). The color code given at the top of the figure distinguishes the S1-S4 SPEs (there were no S5 events in the sample). Open circles below the contour indicate correct null forecasts while those above indicate False Alarms (FAs). The forecast statistics for the 20-yr interval, as determined by Alberti et al. (2017), are as follows:

- POD = Hits/ (Hits + Misses + MISSES) = 66/(66+20+21)=62%
- FAR = FAs/(Hits + FAs)= 42/(66+42)=39%

For ≥S1 events, the SPE alert is issued 10 minutes after the ≥M2 SXR peak and the SPE onset is the end of the third consecutive 5-min interval for which the average >10 MeV flux is ≥10 pfu. The positive difference between these two times is the forecast warning time. The median warning time for the hits in our sample of ≥S1 events for this 20-yr interval was 4.8 h with a range from 0.4 to 52.8 h.

3.2. *ESPERTA applied to ≥S2 (≥100 pfu) events*

It can be observed in Figure 2 that the majority of S1 events (blue symbols), correspond to quite low values of SXR and radio fluence. Many of them are Misses (blue stars, 15/38) in ESPERTA. On the contrary, the majority of ≥S2 SPE events (green, red and yellow symbols) have high values of SXR and radio fluence, with very few misses (green and red stars, 5/47). Thus if we use ESPERTA to predict ≥S2 events, we can eliminate 15 events that are not predicted (blue stars in Figure 2). These 15 events now become correct null forecasts (open circles below the contours).

Additional revisions to ESPERTA can further enhance its performance for predicting ≥S2 events as shown in Figure 3. First, the ESPERTA probability contours are optimized for forecasting such events for the three longitude ranges: that for the W20-W120 longitude bin is adjusted upward from a parameter value of 0.28 to 0.35 while the contours for the other two bins are left unchanged. This results in the conversion of 11 hits (blue squares, the S1 events whose SXR and radio fluences are placed between 0.28 and 0.35 contours) in Figure 2 into correct null forecasts (open circles below the 0.35 contour) in 3. On the other hand, the one red and one green square between the contours become stars, i.e., Missed events.

A further refinement of the ESPERTA based forecasting method for ≥S2 events is more significant: alerts are only issued for SPEs that have reached the S1 level, rather than for all ≥M2 flares. This change has the immediate advantage that the 36 ≥M2 events that triggered forecasts that were false alarms (open circles above the contour lines) in Figure 2 are discarded in Figure 3, i.e., no forecast will be made. This gain is offset by the corresponding conversion of the 12 blue squares above the probability contours in Figure 2 to open circles (false alarms) in Figure 3.

The net result of these various modifications associated with the application of ESPERTA to ≥S2 SPEs for 1995-2014 (Figure 3) is a significant improvement of forecast statistics over those obtained for classical ESPERTA for ≥S1 events.

- POD = Hits / (Hits + Misses + MISSES) = 41/(41 + 7 + 6) = 76%
- FAR = FAs / (Hits + False Alarms) = 12 / (41 + 12) = 23%

One parameter that does not improve for ESPERTA ≥S2 vs. ≥S1 predictions is the warning time (difference between columns 12 and 13 in Table 2) which is reduced over all, with median value of ∼1.2 h and a range from ∼0.2 to 54.8 hours. The distribution of warning times for the 41 hits for ≥S2 SPEs in our sample is shown in Figure 4. Five events (Nos. 25, 44, 46, 58, and 59, in Table 2) had delays ranging from ∼20-55 h. The associated longitude range of the eruptions was E89-W06. For four of these cases, the >10 MeV intensity rose gradually from the S1 threshold to the S2 threshold (see Figure 1). For the fifth case (No. 58: E82, 54.8 h warning time), the ≥100 pfu threshold was reached via a shock spike superimposed on the SPE event. For such cases, advance warning may be also possible based on satellite observations at L1 (Cohen et al. 2001).

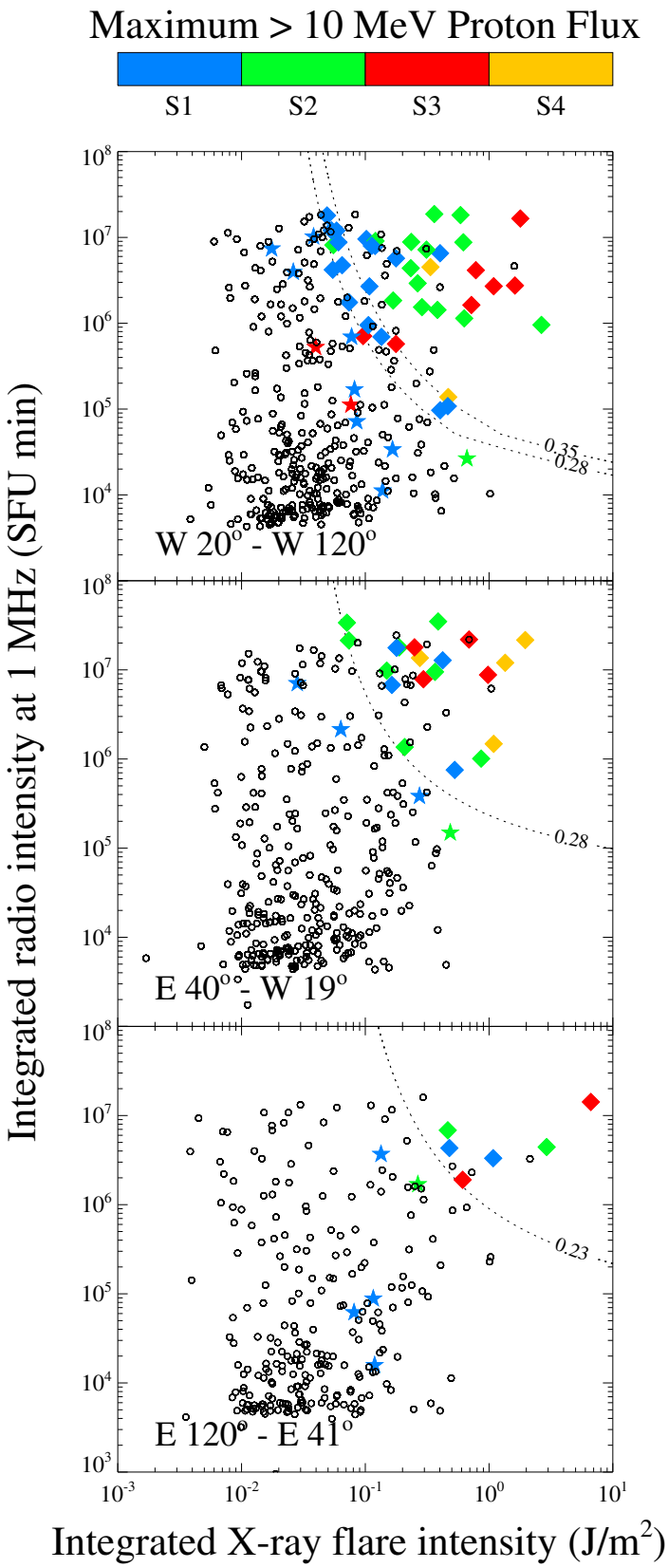

Figure 2. ESPERTA probability contours for prediction of ≥S1 SPEs for three solar longitude bands. Symbols: open circles outside contours = correct null forecasts; open circles inside contours = false alarms; stars = ≥S1 SPEs not predicted (Misses); squares = correctly predicted ≥S1 SPEs (Hits). Color coding gives the NOAA Radiation Storms scale (Table 1).

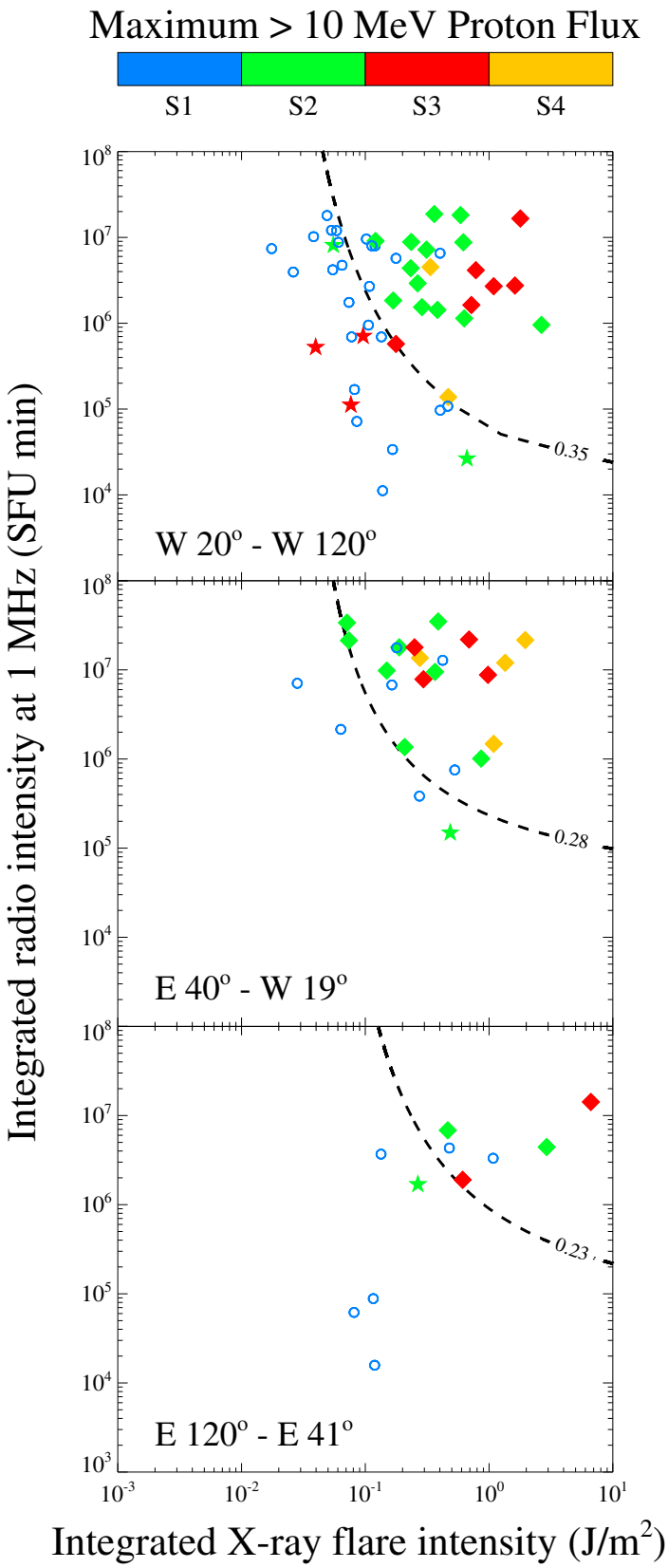

Figure 3. ESPERTA probability contours for prediction of ≥S2 SPEs for three solar longitude bands. Symbols: open circles outside contours = correct null forecasts; open circles inside contours = false alarms; stars = ≥S2 SPEs not predicted (Misses); squares = correctly predicted ≥S2 SPEs (Hits). Color coding gives the NOAA Radiation Storms scale (Table 1).

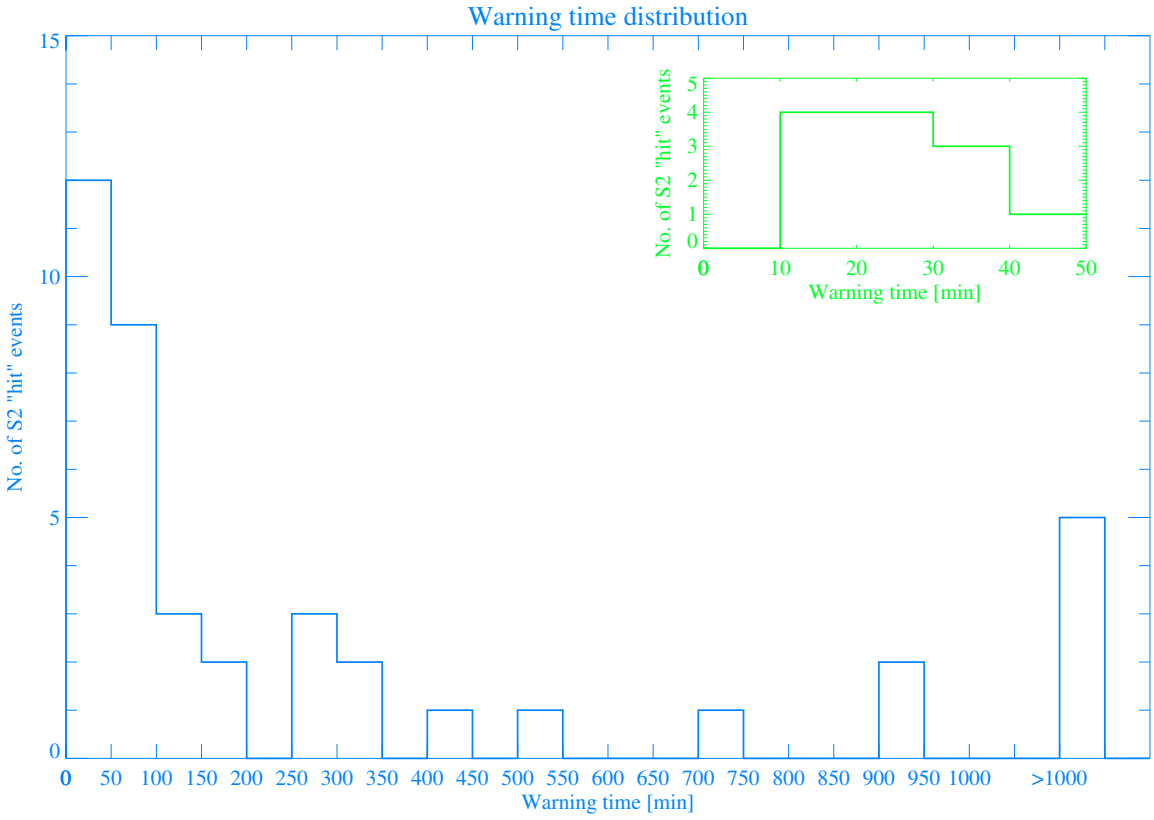

Figure 4. Histogram of warning times for ESPERTA predictions of ≥S2 > 10 MeV proton events. Inset for predicted SPEs with warning times ≤50 minutes.

As discussed below, we attribute the improved performance of ESPERTA for ≥S2 SPEs to a big flare syndrome (Kalher 1982) effect. From 1995 to 2014, CMEs associated with ≥S1 events had a median speed of 1289 km s^{-1} vs. a corresponding value of 1748 km s^{-1} for ≥S2 events. CME kinetic energy is the dominant component in the energy budget of eruptive flares (Emslie et al. 2012).

4. SUMMARY AND CONCLUSION

We applied the ESPERTA alert method of Laurenza et al. (2009) and Alberti et al. (2017), previously used only for the ≥S1 events (with peak >10 MeV proton intensity ≥10 pfu) typically addressed by such techniques, to the more geoeffective ≥S2 events (Table 2), which have a >10 MeV flux threshold of 100 pfu. For the 1995-2014 interval, the POD for ≥S2 events was 76% vs. 62% for ≥S1 events and the FAR was 23% vs. 39%. Larger and more hazardous solar proton events are easier to forecast than the classic ≥S1 events, although on the negative side the median (minimum) warning time for ≥S2 SPEs is reduced to ∼1.2 h (∼0.2 h) vs. 4.8 h (0.4 h) for ≥S1 events. This improvement in the POD and FAR parameters appears to result from a beneficial effect of the big flare syndrome (BFS; Kalher 1982). Normally, the BFS is viewed as a hindrance that makes it difficult to decipher the physics of big flares. For the SPE alert application, however, delaying the forecast of a ≥S2 event until the S1 level is reached provides important new information for the ESPERTA technique as we are now only considering flares with a demonstrated potential to produce base-level SPE impacts, a qualitative input that supplements the consideration of big flares (i.e., large SXR and ∼1 MHz

fluences) in the application of ESPERTA to ≥S1 events. If, generally, the BFS means that big flares have more of everything, then a selection of even bigger flares is more likely to have the attribute of ≥S2 SPE association. Looking ahead, such delayed forecasts of ≥S2 events allow more time to refine the estimated flare SXR and radio inputs currently used for longer-duration flares in ESPERTA and other empirical models. Alternatively, it permits the possibility to use inputs that are thought to be more directly related to the proton acceleration process in eruptive flares (e.g., CME speed and DH type II burst association; Cliver 2004; Gopalswamy et al. 2010) in more physics-based forecast models.

All data used in this analysis are publicly accessible from NASA (Wind/WAVES) and NOAA (GOES). The Wind/WAVES data were obtained from ftp://solar-radio.gsfc.nasa.gov/. GOES data have been downloaded from http://www.ngdc.noaa.gov/stp/satellite/ goes/dataaccess.html.

REFERENCES

Alberti, T., Laurenza, M., Cliver, E. W., Storini, M., Consolini, G., & Lepreti, F. 2017, Astrophys. J., 838, article id. 59, 11 pp

Balch, C. C. 2008, Space Weather, 6, S01001

Barnes, G., Leka, K.D., Schrijver, C.J., Colak, T., Qahwaji, R., Ashamari, O.W., Yuan, Y., et al. 2016, Astrophys. J., 829, article id. 89

Bougeret, J. L., Kaiser, M. L., Kellog, P., Manning, R., Voltz, K. et al 1995, Space Sci. Rev., 71, 231

Cliver, E.W. 2004, Astrophys. J., 605, 902

Cliver, E.W. 2016, Astrophys. J., 832, article id. 128

Cohen, C.M.S., Mewaldt, R.A., Cummings, A.C., Leske, R.A., Stone, E.C., Slocum, P.L., Wiedenbeck, M.E., et al. 2001, J. Geophys. Res., 106, 20979

Emslie, A.G., Dennis, B.R., Shih, A.Y., Chamberlin, P.C., Mewaldt, R.A., Moore, C.S., Share, G. H., et al. 2012, Astrophys. J., 759, article id. 71

Garcia, H. A. 1994, ApJ, 420, 422-432, doi:10.1086/173572.

Gopalswamy, N., Yashiro, S., Michalek, G., Stenborg, G., Vourlidas, A., Freeland, S., & Howard, R. 2009, Earth, Moon, Planets, 104, 295

Gopalswamy, Natchimuthukonar 2010, in Heliophysical Processes, eds., N. Gopalswamy, S. Hasan, A. Ambastha (Springer-Verlag: Berlin), p. 53

Kahler, S.W. 1982, J. Geophys. Res., 87, 3439

Kahler, S.W., Cliver, E.W., & Ling, A.G. 2007, J. Atmos. Sol.-Terr. Phys., 69, 43

Laurenza, M., Cliver, E. W., Hewitt, J., Storini, M., Ling, A., Balch, C. C. & Kaiser, M. L. 2009, Space Weather, 7, S04008, doi:10.1029/2007SW000379

Laurenza, M., Hewitt, J., Cliver, E. W., Storini, M. & Ling, A. 2007, Solar energetic proton events and soft X-ray flares, paper presented at 20th Eur. Cosmic Ray Symp. 2006, Lisbon 5-8 Sept. (Available online at http://www.lip.pt/events/2006/ecrs/proc/ecrs06-s1-34.pdf.)

Marubashi, K., Akiyama, S., Yashiro, S., Gopalswamy, N., Cho, K.-S., & Park, Y.-D. 2015, Solar Phys., 290, 1371

McCullagh, P. & Nelder, J. A. 1983, Generalized Linear Models, chap. 4, pp. 98-155, Chapman and Hall, London

Núñez, M. 2011, Space Weather, 9, S07003

Papaioannou, A., Anastasiadis, A., Sandberg, I., Georgoulis, M.K., Tsiropoula, G., Tziotziou, K., Jiggens, P. & Hilgers, A. 2015, J. Physics: Conference Series, 632, 012075

Papaioannou, A., Sandberg, I., Anastasiadis, A., Kouloumvakos, A., Georgoulis, M. K., Tziotziou, K., Tsiropoula, G., Jiggens, P., & Hilgers, A. 2016, J. Space Weather Space Clim., 6, A42, doi:10.1051/swsc/2016035

Posner, A. 2007, Space Weather, 5, S05001

Reames, D. V. 1999, Space Sci. Rev., 90, 413-491

Reames, D.V. 2013, Space Sci. Rev., 175, 53

Reames, D.V. 2017, Solar Energetic Particles, Springer, Heidelberg

Signoretti, F., Laurenza, M., Marcucci, M. F. & Storini, M. 2011, Proceedings of the 32nd International Cosmic Ray Conference (Beijing, China, 11 - 18 August 2011), 10, 267-270

Silverman, B. W. 1998, CRC Press, Boca Raton

St. Cyr, O. C., Posner, A. & Burkepile, J. T. 2017, Space Weather, 15, 240-257, doi:10.1002/2016SW001545

Storini, M., Cliver, E. W., Laurenza, M. & Grimani, C. 2008, OPOCE publisher for COST 724 action, 63-69

Winter, L. M. & Ledbetter, K. 2015, ApJ, 809:105 (19pp)

Yashiro, S., Gopalswamy, N., Michalek, G., St. Cyr, O.C., Plunkett, S.P., Rich, N.B., & Howard, R.A. 2004, J. Geophys. Res., 109, CiteID A07105